Interaction of the UvrABC Nuclease System with a DNA Duplex Containing a Single Stereoisomer of dG-(+)- or dG-(−)-*anti*-BPDE†

Yue Zou,‡ Tong-Ming Liu,§ Nicholas E. Geacintov,§ and Bennett Van Houten*,‡

Sealy Center for Molecular Science, University of Texas Medical Branch, Galveston, Texas 77555, and Department of Chemistry, New York University, New York, New York 10003

Received June 2, 1995; Revised Manuscript Received August 8, 1995⊗

ABSTRACT: Oligonucleotides containing site-specifically-modified N^2-guanine (+)-*trans*-, (−)-*trans*-, (+)-*cis*-, and (−)-*cis*-BPDE adducts were ligated into 50-base-pair DNA fragments. These substrates were used in reactions with the *Escherichia coli* UvrABC nuclease system. The interaction of the $UvrA_2$ and $UvrA_2B$ complexes with these four stereoisomers was probed using DNase I footprinting and gel mobility shift assays. DNase I digestion of substrates containing each stereoisomer of BPDE displayed a unique pattern which was consistent with the known structure of these DNA adducts. UvrA and $UvrA_2B$ appeared to interact very similarly with all four substrates. Binding of $UvrA_2$ to these substrates produced a 33-bp footprint, and the UvrB−DNA complex resulted in footprint of 24 bp. The UvrABC nuclease system produced bimodal incisions at the eighth phosphate 5′ and the fifth, sixth, or seventh phosphate 3′ to the modified guanine. The variation of the 3′ incision site was linked to the stereochemistry and orientation of the BPDE adduct. For example, the 3′ incision of the 50-bp duplex containing (−)-*trans*-BPDE-N^2-guanine was inhibited at the fifth phosphate. UvrABC nuclease incision kinetics revealed a hierarchy of specificity. The intercalative *cis* isomers were incised more efficiently than the corresponding *trans* isomers which lie in the minor groove. The (+) enantiomers were incised more efficiently than the (−) form for both *cis* and *trans* isomers. These observations reveal that UvrABC nuclease recognition and incision are directly influenced by the conformation of the DNA adduct.

The ability of a protein or protein complex to bind specific DNA damage represents an important structure-specific form of protein−DNA interaction. DNA damage recognition proteins of the nucleotide excision repair (NER)[1] pathway are interesting because they can act on a large number of DNA adducts which are chemically and structurally distinct. The questions arise, how are damage-induced conformational changes in the DNA helix perceived by a DNA repair protein complex, and how is this recognition translated through protein−DNA contacts into higher binding affinities and increased incision efficiencies? The *Escherichia coli* UvrABC nuclease is an excellent system in which to address this question.

The UvrABC nuclease system initiates NER through a series of integrated steps which culminate by scission of the damage-containing strand at two discrete sites [reviewed in Van Houten (1990) and in Van Houten and McCullough (1994)]. UvrA (103.8 kDa) exists in equilibrium between a monomer and dimer in solution (Oh & Grossman, 1986; Mazur & Grossman, 1991). $UvrA_2$ binds to UvrB (76.6 kDa) to form a heterotrimer, $UvrA_2B$ (Orren & Sancar, 1989a,b, 1990). This $UvrA_2B$ complex has been shown to have limited DNA helicase activities (Oh & Grossman, 1989; Moolenaar *et al.*, 1994) and in an ATP-dependent manner can induce negative and positive supercoiling waves within plasmid DNA (Koo *et al.*, 1991). It is believed that the $UvrA_2B$ complex, through the energy of ATP hydrolysis, may travel along the DNA in an active search for conformational perturbations induced by DNA damage (Grossman & Thiagalingam, 1993). Upon encountering a damaged site, allosteric changes in the protein−DNA complex occur, leading to a conformational change in the DNA and a concomitant change in the affinity of the $UvrA_2$ for the damaged site (Orren & Sancar, 1990). Dissociation of $UvrA_2$ results in a stable UvrB−DNA complex which serves as a scaffold for the binding of UvrC (68.1 kDa). An ensuing allosteric change in UvrB activates an intrinsic nuclease which appears to cleave the phosphate backbone four nucleotides 3′ to the damaged base (Linn *et al.*, 1992). This reaction serves to trigger a nuclease within UvrC which hydrolyzes a phosphate seven nucleotides 5′ to the damaged site (Sancar & Rupp, 1983; Linn & Sancar, 1992). The dual action of DNA helicase II and DNA polymerase I work to dissociate the UvrBC−DNA postincision complex and fill in the resulting gap. NER is completed by the action of DNA ligase which seals the nick left at the 3′ side of the 12-nucleotide repair patch.

One of the most remarkable aspects of the UvrABC system is its broad substrate repertoire acting on a variety of DNA

† This work was supported by the Sealy Center for Molecular Science and Department of Energy Office of Health and Environmental Research, Grant DE-FGO2-86ER60405 (N.E.G.).

* Author to whom all correspondences should be sent, at Sealy Center for Molecular Science, 5th floor MRB, University of Texas Medical Branch, Galveston, TX 77555-1071. Tel.: (409) 772-2144. FAX: (409) 772-1790.

‡ University of Texas Medical Branch.

§ New York University.

⊗ Abstract published in *Advance ACS Abstracts,* October 1, 1995.

[1] Abbreviations: BPDE, benzo[*a*]pyrene diol epoxide, 7,8-dihydroxy-9,10-epoxy-7,8,9,10-tetrahydrobenzo[*a*]pyrene; (+)-*anti*-BPDE, (7*R*,8*S*)-dihydroxy-(9*S*,10*R*)-epoxy-7,8,9,10-tetrahydrobenzo[*a*]pyrene; (−)-*anti*-BPDE, (7*S*,8*R*)-dihydroxy-(9*R*,10*S*)-epoxy-7,8,9,10-tetrahydrobenzo-[*a*]pyrene; BSA, bovine serum albumin; DTT, dithiothreitol; EDTA, ethylenediaminetetraacetic acid; NER, nucleotide excision repair; PAGE, polyacrylamide gel electrophoresis; TBE, tris−borate EDTA.

0006-2960/95/0434-13582$09.00/0 © 1995 American Chemical Society

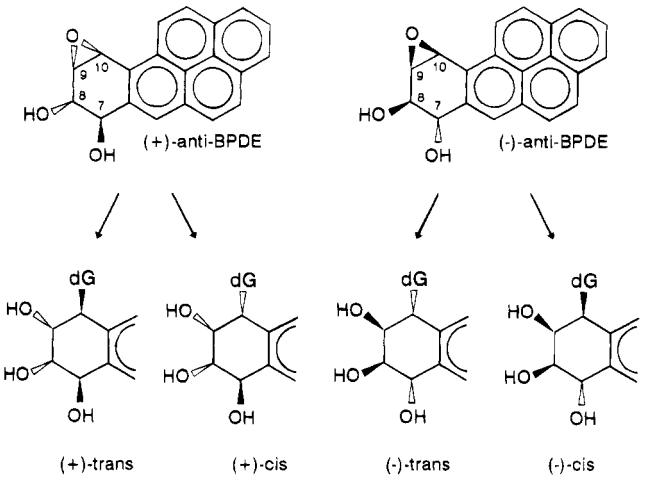

FIGURE 1: Structures of (+)-*trans*-, (−)-*trans*-, (+)-*cis*-, and (−)-*cis*-*anti*-benzo[*a*]pyrene diol epoxide (BPDE) stereoisomers used in the present study.

lesions which differ widely in chemical composition, structure, and effect on DNA conformation (Van Houten, 1990; Van Houten & Snowden, 1993). One of the challenges in understanding how the UvrABC system can identify damaged bases is the limited number of high-resolution structures of DNA adducts. This problem is compounded by the need to place the damaged nucleotides in a defined sequence context so that direct comparisons among different types of adducts can be made. An ideal substrate for the UvrABC nuclease system would consist of a family of DNA adducts with identical or closely related chemistry which produce different types of conformational changes in the DNA helix. One such family of DNA adducts are those which result from the interaction of the benzo[*a*]pyrene diol epoxide (BPDE), the active metabolite of the ubiquitous environmental pollutant benzo[*a*]pyrene, with DNA.

The stereochemical attack of the C^{10}-epoxide of either the (+)- *or* (−)-*anti*-BPDE at the N^2-position of guanine adducts results in two pairs of enantiomeric adducts: (+)-*trans*-, (+)-*cis*-, (−)-*trans*-, and (−)-*cis*-BPDE-N^2-guanine, respectively (Figure 1). The structures of 11-bp DNA duplexes containing either (+)-*trans*-, (+)-*cis*-, or (−)-*trans*-BPDE-N^2-guanine adducts, which have been placed site-specifically within the same sequence context, have been solved using a combined technique of energy minimization and distance constraints obtained from 2D-NMR experiments (Cosman *et al.*, 1992, 1993; de los Santos *et al.*, 1992). These remarkable structures have shown that the (+)-*trans*- and (−)-*trans*-BPDE-N^2-guanine adducts lie in the minor groove, with the benzo[*a*]pyrene moiety oriented in the 5′ and 3′ directions, respectively, with respect to the modified G (Cosman *et al.*, 1992; de los Santos *et al.*, 1992). In contrast, both *cis*-BPDE-N^2-dG adducts assume a base-displacement intercalative conformation in which the aromatic BPDE residues stack with the neighboring bases on the same strand; the modified guanine and partner cytidine residue on the complementary strand are displaced into the minor and major grooves, respectively, in the case of the (+)-*cis* adduct (Cosman *et al.*, 1993), while both of these residues are displaced into the major groove in the case of the (−)-*cis* adduct (M. Cosman, private communication, 1995).

It is not unexpected that these differences in conformation result in different biological effects. For example, the (+)-*anti*-BPDE isomer is more tumorigenic than the (−)-*anti*-BPDE isomer when applied to mouse skin or the lungs of newborn mice (Slaga *et al.*, 1979; Buening *et al.*, 1978). The (+)-*anti*-BPDE isomer is more mutagenic than the chiral (−)-isomer in mammalian cells (Wood *et al.*, 1977; Wei *et al.*, 1994), but the reverse order of activities is observed in bacterial cells (Wood *et al.*, 1977; Steven *et al.*, 1985). More recently oligonucleotides containing stereospecific and site-specifically-placed BPDE-N^2-dG lesions were used as templates in primer extension reactions catalyzed by *E. coli* Pol I (Klenow fragment, exonuclease free); the mutagenic potential of the lesions derived from (−)-*anti*-BPDE displayed a significantly higher miscoding potential than those derived from the (+)-enantiomer in this *in vitro* site-directed mutagenesis assay (Shibutani *et al.*, 1993). In these (Shibutani *et al.*, 1993) and other primer extension experiments with site-specific oligonucleotides (Hruszkewicz *et al.*, 1992), the BPDE-N^2-dG lesions are efficient blocks of the DNA polymerases. Choi *et al.* (1994) found that T7 RNA polymerase is also strongly inhibited by *anti*-BPDE-N^2-dG adducts, the order of inhibition being (+)-*trans*- > (−)-*trans*- > (+)-*cis*- > (−)-*cis*-BPDE-N^2-guanine.

The interaction of DNA repair enzymes with these defined substrates has not been examined previously. In this present report we examine the interaction of the UvrABC nuclease system with DNA duplexes containing site-specifically-placed (+)-*trans*-, (−)-*trans*-, (+)-*cis*-, and (−)-*cis*-BPDE-N^2-guanine. DNase I footprinting and gel mobility shift assays have been used to examine the interaction of the UvrA and $UvrA_2B$ complexes with the DNA substrates. The 5′ and 3′ incision sites of the UvrABC nuclease system was monitored by DNA sequencing gel analysis. Our results provide direct evidence that incision kinetics and the 3′ incision sites are affected by the specific conformation of the BPDE-N^2-guanine adduct.

MATERIALS AND METHODS

Chemicals. Tris base, boric acid, ethylenediaminetetraacetic acid (EDTA), and $CaCl_2$ were purchased from Sigma. Acrylamide, ammonium persulfate, *N,N′*-methylenebisacrylamide, and urea were obtained from Bethesda Research Laboratories (BRL). [γ-^{32}P]ATP and [α-^{32}P]-cordycepin-5′-triphosphate (DuPont) were purchased from New England Nuclear Inc. Racemic BPDE was purchased from the National Cancer Institute Chemical Carcinogen Reference Standard Repository.

Purification of UvrA, UvrB, and UvrC Proteins. UvrA was purified from *E. coli* strain MH1 ΔUvrA containing the overproducing plasmid, pSST10 (graciously supplied by L. Grossman, Johns Hopkins University), which is under the control of the heat-inducible PL promoter. UvrB and UvrC were overproduced from *E. coli* strain CH296 containing plasmids pUNC211 and pDR3274, respectively (graciously supplied by A. Sancar, University of North Carolina). The UvrB and UvrC proteins were purified as described previously (Sancar *et al.*, 1987). UvrA was purified to homogeneity using a new procedure. Briefly, a cell-free sonicate was eluted through a Q-sepharose column and directly into a single-strand DNA cellulose column connected in tandem. UvrA was eluted using a KCl gradient and appeared at approximately a 170 mM KCl. Fractions containing UvrA were pooled and dialyzed into a buffer containing 25 mM KCl, 20 mM Tris·HCl (pH 8.0), 20 mM KPO_4 (pH 8.0), 1 mM EDTA, 10 mM β-mercaptoethanol, and 10% glycerol and injected onto a Mono-Q FPLC column. UvrA eluted at

BPDE 50mer Substrate:

```
          20mer          |  11mer   |  19mer
5'-GACTACGTACTGTTACGGCTCCATCGCTACCGCAATCAGGCCAGATCTGC-3'
3'-CTGATGCATGACAATGCCGAGGTAGCGATGGCGTTAGTCCGGTCTAGACG-5'
          .    .    .    .    .    .    .    .    .    .
          5    10   15   20   25   30   35   40   45   50
```

FIGURE 2: Construction of BPDE−50-bp DNA substrates. The 11mer containing a single BPDE stereoisomer (G) was ligated with a 19mer and a 20mer in the presence of the 50mer complementary strand. The recognition sequences of restriction endonuclease are indicated by underlines.

approximately 195 mM KCl. In a final step of purification UvrA was separated from minor lower molecular weight contaminants by gel filtration on a G-200 FPLC columns. All proteins were stored at −80 °C in storage buffer containing 50 mM Tris·HCl (pH 7.5), 100 mM KCl, 1 mM EDTA, 1 mM DTT, and 50% glycerol. Preparations of the Uvr proteins (5.0 μg) analyzed by SDS−PAGE and stained by Coomassie blue gave a single band. These proteins had no detectable nonspecific endo or exo nuclease activities. Concentrations of the Uvr proteins were determined by the Bio-Rad protein assay using BSA as a standard following the manufacturer's suggested protocol.

Other Enzymes. All restriction and modifying enzymes were obtained from Promega or New England Biolabs unless otherwise indicated.

DNA Oligodeoxynucleotides. Oligomers used in this study were either obtained from OPERON or synthesized on an Applied BioSystems 394 DNA/RNA synthesizer. All products were purified by PAGE under denaturing conditions. The four oligodeoxynucleotide 11mers (Figure 2) containing (+)-*trans*-, (−)-*trans*-, (+)-*cis*-, and (−)-*cis*-*anti*-benzo[*a*]-pyrene (BPDE) stereoisomers, respectively, were synthesized, purified, and characterized as described previously (Cosman *et al.*, 1991).

Preparation of anti-BPDE-Modified 50-bp DNA Duplexes. In order to obtain BPDE-N^2-dG-adducted 50-bp substrates (Figure 2), the phosphorylated BPDE−11mers (20 pmol) were incubated with equal moles of the 20mer (5′-terminally-labeled with ^{32}P), the phosphorylated 19mer, and the bottom strand 50mer in a 30 μL solution containing 50 mM Tris·HCl, pH 7.8, 10 mM $MgCl_2$, 10 mM DTT, 1 mM ATP, and 50 μg/mL of BSA. The mixture was brought to 75 °C for 5 min and was then slowly cooled down to room temperature and finally to 16 °C, followed by adding 0.2 units of T4 DNA ligase. The ligation was carried out at 16 °C for 12 h. The sample was reheated at 80 °C for 5 min with 8 M urea followed by rapidly chilling on ice and then purified on a 12% (w/v) polyacrylamide sequencing gel under denaturing conditions in a TBE (50 mM Tris, 50 mM boric acid, 1 mM EDTA, pH 8) buffer. The band identified as BPDE−50mer by autoradiography with Kodak XAR5 X-ray film was excised, eluted, and precipitated with ethanol. After being resuspended in TEN buffer (10 mM Tris·HCl, pH 8.0, 100 mM NaCl, 1 mM EDTA), the nondamaged or adducted 50mer DNA strand (top, Figure 2) was annealed with the complementary strand (bottom strand, Figure 2) by heating at 80 °C for 5 min and then slowly cooling down to room temperature followed by at least three additional hours of incubation. The sample was electrophoresed in a 10% (w/v) polyacrylamide nondenaturing gel with TBE buffer and purified as described above.

The double-stranded character and homogeneity of the 50-bp substrates were examined by a restriction assay in which the substrate (1 nM) was incubated with *Rsa*I or *Hae*III (20 units) at 37 °C for 30 min. The reaction was terminated by heating at 70 °C for 10 min. Samples were then analyzed on a 12% (w/v) polyacrylamide sequencing gel under denaturing conditions as described below. To examine the nature of the chromophore in the 50-bp duplex containing the BPDE-N^2-guanine adduct, excitation (em = 400 nm) and emission (ex = 350 nm) spectra were recorded with a Hitachi F-4500 fluorometer with slits (ex/em) of 5.0 nm/5.0 nm, PMT voltage of 700 V, and a response of 0.01 s. The concentration of the BPDE-adducted 50-bp duplex DNA was determined using $\epsilon_{260} = 660\,000\ M^{-1}\ cm^{-1}$, and the radioactive specificity of the substrate was measured with a liquid scintillation counter (Beckman LS6000SC).

Preparation of the 3′-terminally-labeled substrates was conducted in the same way as that for 5′-end-labeled except that the oligonucleotide 19mer was 3′-terminally-labeled with [α-^{32}P]cordycepin-5′-triphosphate and terminal transferase. Sequencing of the 5′- or 3′-terminally-labeled (^{32}P) 50-bp DNA duplex was performed using standard Maxam−Gilbert procedures (Maxam & Gilbert, 1980) with a DuPont NEN sequencing kit.

Binding of UvrA and UvrB to BPDE−DNA Substrates. The binding of DNA repair proteins UvrA and UvrB to the BPDE-damaged DNA substrate was qualitatively examined by gel mobility shift assay. Typically, 5′- or 3′-end-labeled DNA substrate (1 nM) was incubated with UvrA (2−10 nM) or/and UvrB (200 nM) at 37 °C for 15 min in 20 μL of UvrABC buffer (50 mM Tris·HCl, pH 7.5, 50 mM KCl, 10 mM $MgCl_2$, 5 mM DTT, 1 mM ATP). After the incubation, 2 μL of 80% (v/v) glycerol was added and the mixture was immediately loaded onto a 4% or 6% (w/v) native polyacrylamide gel (80:1) running with TBE buffer containing 1 mM ATP and 10 mM $MgCl_2$. The gel was run at 35−40 mA for 2.5−3 h at room temperature. After electrophoresis the gel was dried and exposed for an appropriate time to a Kodak XAR5 X-ray film with an intensifying screen at −70 °C.

DNase I Footprinting. DNase I footprinting was used to determine the number of base pairs contacted by UvrA and UvrB binding to BPDE−DNA. In these reactions the 5′- or 3′-terminally-labeled DNA (2 nM) was incubated with UvrA (50 nM) alone or UvrA (10 nM) plus UvrB (200 nM) subunits in 20 μL of UvrABC buffer for 15 min at 37 °C to allow equilibration. DNase I reactions were initiated by the addition of 2 μL of 0.1 M $CaCl_2$ at room temperature and 1 ng of DNase I (Sigma). The reaction proceeded for 60 s and was then terminated by adding 20 mM EDTA and heating to 90 °C for 3 min. The samples were mixed with 20 μL of formamide (98%) DNA-denaturing buffer and heated to 90 °C followed by immediately chilling on ice. Along with Maxam and Gilbert (1980) sequence products, samples were electrophoresed in a 14% (w/v) polyacrylamide sequencing gel (8 M urea) under denaturing conditions with TBE buffer (50 mM Tris, 50 mM boric acid, 1 mM EDTA, pH 8). The gel was dried and exposed to Kodak XAR5

X-ray film with intensifying screen at −70 °C from 1 to 4 days.

UvrABC Incision. The 5′- or 3′-terminally-labeled BPDE−DNA substrate (1 nM) was digested with UvrA (10 nM), UvrB (100 nM), and UvrC (5 nM) in a 20 μL reaction buffer containing 50 mM Tris·HCl, pH 7.5, 50 mM KCl, 10 mM $MgCl_2$, 5 mM DTT, and 1 mM ATP at 37 °C for 5−20 min. Maximum incision efficiency was achieved when all three Uvr subunits were diluted and premixed into storage buffer prior to mixing with DNA. The reaction was terminated by adding EDTA (20 mM) and heating to 90 °C for 3 min. The samples were denatured with formamide (50% v/v) and heated to 90 °C and then quick-chilled on ice. The digested products were loaded onto a 12% (w/v) polyacrylamide sequencing gel under denaturing conditions with TBE buffer. The gel was dried and visualized as described above.

Quantification of Incision Products. In this study, all quantitative data of radioactivity were generated using PhosphorImager 425 (Molecular Dynamics), and IMAGEQUANT software (Molecular Dynamics) using the volume integration method. The amount of DNA incised (DI, in pmol) by UvrABC was calculated based on the total molar amount of DNA used in each reaction (M) and the percentage of radioactivity in the incision products (IP) as compared to the total radioactivity in both the 50mer and incision products using the formula $DI_{total} = [IP/(50mer + IP)]M$.

RESULTS

Construction of the BPDE−50-bp DNA Duplex. In order to investigate the interaction of *E. coli* UvrABC DNA repair proteins with BPDE-damaged DNA, a defined sequence of 50-bp oligodeoxynucleotides containing a single BPDE adduct was prepared with the four *anti*-BPDE stereoisomers. The substrates were constructed by ligating a single BPDE-modified 11mer with a flanking 20mer and a 19mer oligonucleotide on the 5′ and 3′ sides, respectively, in the presence of the 50mer complementary strand (Figure 2). Relatively mild conditions (e.g., DNA denatured at 80 °C with urea instead of at >90 °C with formamide) were used to prevent BPDE from undergoing any potential chemical alternation during the preparation. All sample preparation conditions were tested by examining the excitation and emission spectra of a BPDE−11mer before and after being subjected to identical conditions. Following the denaturing and annealing steps, the ligation was performed with T4 DNA ligase at 16 °C for at least 12 h and then purified on a 12% polyacrylamide denaturing gel. As shown in Figure 3A for the products of a typical ligation of the oligomers with the 5′-terminally-labeled 20mer, the ligation efficiencies for the five substrates are quite different, although good yields of ligation have been obtained for all. Nondamaged DNA substrate (lane 1) always showed the highest ligation efficiency in our preparations, followed by (+)-*cis*- (lane 4), (−)-*trans*- (lane 3), (+)-*trans-anti*-BPDE−DNA (lane 2), and the (−)-*cis* isomer (lane 5). After the purification, the ligated 50mer was reannealed with the complementary strand (bottom strand) and purified again on a 10% polyacrylamide native gel as shown in the Figure 3B. To confirm that all the substrates were fully double stranded and homogenous, they were digested with the restriction enzyme *Rsa*I (Figure 3C) or *Hae*III (data not shown). *Rsa*I specifically recognizes the palindromic sequence d(GTAC)·d(CATG) and digests these substrates into an 8mer and a 42mer. All substrates were digested to >95% (Figure 3C) as indicative of loss of the 50mer band accompanied by appearance of the 8mer band (lanes 2, 4, 6, 8, and 10). The restricted 42mer is invisible since the samples shown in Figure 3 were all 5′-terminally labeled.

The fluorescence properties of the purified BPDE-modified duplex were examined to ensure that the benzo[*a*]pyrene chromophore remains intact during the preparation steps. Both the excitation (em = 400 nm) and emission (ex = 350 nm) spectra were recorded for each of the four substrates and were typical for BPDE-adducted duplex DNA. Spectra for the (−)-*trans*-BPDE−50-bp DNA, as shown in Figure 4, reveal two well-resolved excitation maxima at 328 and 346 nm and two emission maxima at 382 and 400 nm. The spectra are consistent with those previously reported (Geacintov *et al.*, 1982), indicating the BPDE structures remain unchanged during the substrate preparation. The shift of the excitation maxima from 350 nm for single-stranded *trans*-BPDE 11mer to 346 nm for the 50-bp substrate also verifies that the duplexes have annealed correctly (Geacintov *et al.*, 1991; Ya *et al.*, 1994).

Binding of UvrA and UvrB to Damaged and Nondamaged DNA Substrates. A working model of *E. coli* nucleotide excision repair proposes that several different protein−DNA complexes form during DNA damage recognition (Van Houten & Snowden, 1993). In order to examine whether these intermediates can form between BPDE-damaged DNA and the Uvr repair proteins, a gel mobility shift assay has been used in this study as a simple and direct approach. The substrates used were prepared as described above and include nondamaged 50-bp duplex as control, (+)- and (−)-*trans-anti*-BPDE, and (+)- and (−)-*cis-anti*-BPDE-modified 50-bp DNA. As shown in Figure 5 (panels A and C), incubation of the control and BPDE-damaged substrates (1 nM) with UvrA produces a shifted complex which is consistent with the $UvrA_2$−DNA complex (lanes 5, 6, 9, 10, 13, 14, 17, and 18) (Mazur & Grossman, 1991; Visse *et al.*, 1992; Van Houten & Snowden, 1993). The unshifted band represents the substrate free of proteins. UvrA shows a high degree of specificity, binding to the BPDE−DNA substrates with high affinity and showing little or no binding to the nondamaged 50-bp duplex. Highly overexposed X-ray films of the gel show a small amunt of UvrA (10 nM) binding to nondamaged DNA (data not shown). Semiquantitative binding isotherms using gel mobility shift assays reveal equilibrium dissociation constants, K_D, in the range of $(10-30) \times 10^{-9}$ M for UvrA binding to each of the four substrates (data not shown).

Interaction of UvrA in the presence of an excess of UvrB (200 nM) (lanes 3, 4, 7, 8, 11, 12, 15, 16, 19, and 20), with all of the BPDE-damaged substrates, resulted in two new shifted complexes which migrate differently from the $UvrA_2$−DNA complex which is formed in the presence of only UvrA (lanes 5, 6, 9, 10, 13, 14, 17, and 18). These intermediates are assigned to be the complexes of UvrB−DNA (migrating much more rapidly than $UvrA_2$-DNA) and $UvrA_2B$−DNA (running more slowly than $UvrA_2$−DNA) (Visse *et al.*, 1992; Van Houten & Snowden, 1993). It is interesting to note that when the same reactions are loaded onto either a 6% (panels A and C) or a 4% (panel B) acrylamide gel the relative abundance of the $UvrA_2B$−DNA and UvrB−DNA complex changes dramatically (lanes 8, 12, 16, and 20). Apparently the higher percentage acrylamide

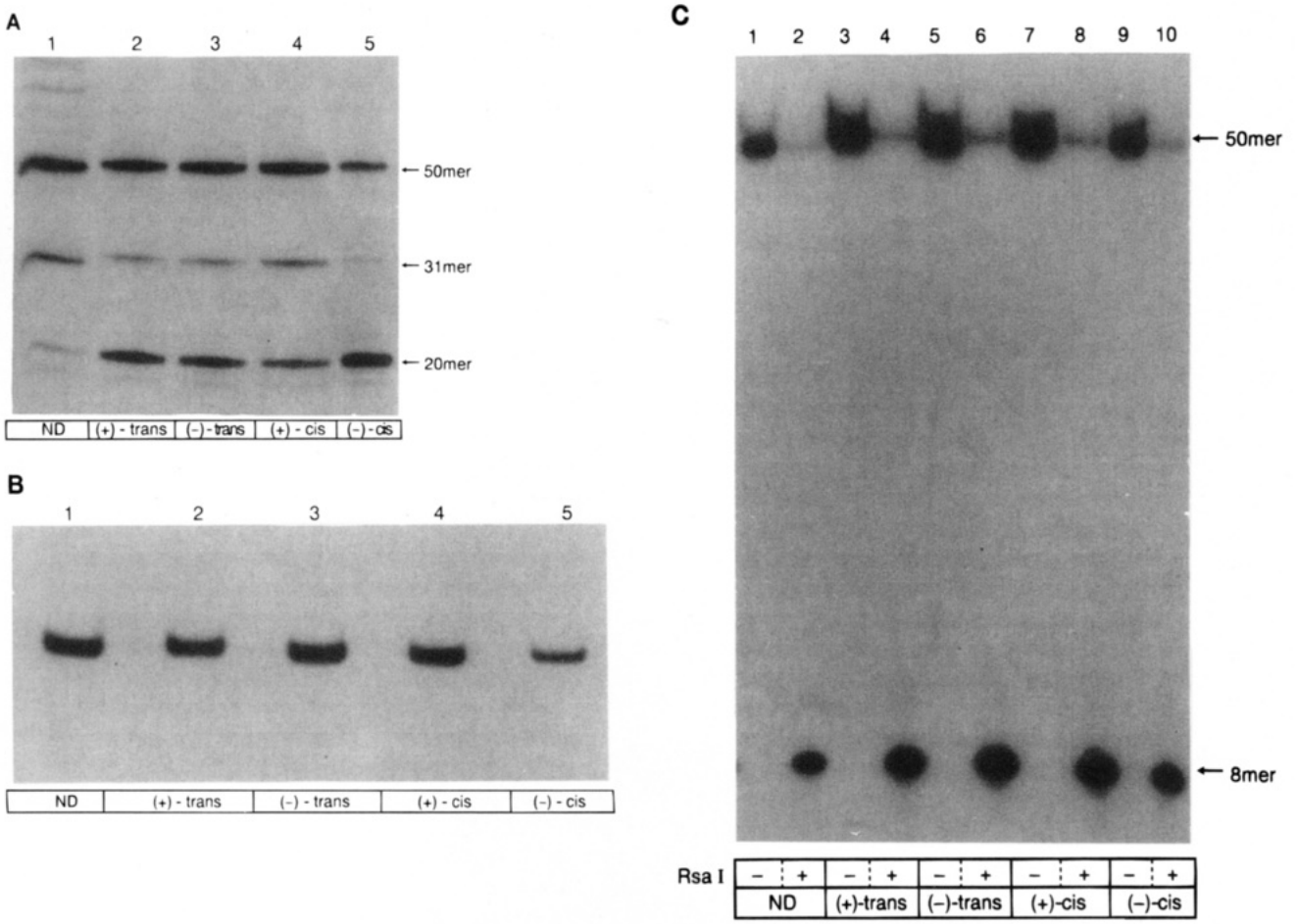

FIGURE 3: Preparation of BPDE−50-bp DNA substrates. Panel A: products of ligation of the BPDE containing the 11mer with a 19mer and a 5′-terminally-labeled 20mer oligonucleotides as purified on a 12% polyacrylamide sequencing gel under denaturing conditions. Lanes 1−5: the ligation with 11mer containing no adduct, (+)-*trans*-, (−)-*trans*-, (+)-*cis*-, (−)-*cis*-anti-BPDE, respectively. Panel B: products of the constructed 50mer hybridized with its complementary strand purified in a 10% polyacrylamide native gel. Lanes 1−5: the constructed 50mer containing no adduct, (+)-*trans*-, (−)-*trans*-, (+)-*cis*-, (−)-*cis-anti*-BPDE, respectively. Panel C: *Rsa*I restriction endonuclease digestion of the constructed 50-bp substrates. The restriction produces a 8mer (5′-labeled) and a 42mer (unlabeled) of the modified strand. Lanes 1, 3, 5, 7, and 9: the unrestricted substrate containing no adduct, (+)-*trans*-, (−)-*trans*-, (+)-*cis*-, and (−)-*cis-anti*-BPDE, respectively. Lanes 2, 4, 6, 8, and 10, the restriction products of the substrates containing no adduct, (+)-*trans*-, (−)-*trans*-, (+)-*cis*-, and (−)-*cis*-BPDE, respectively.

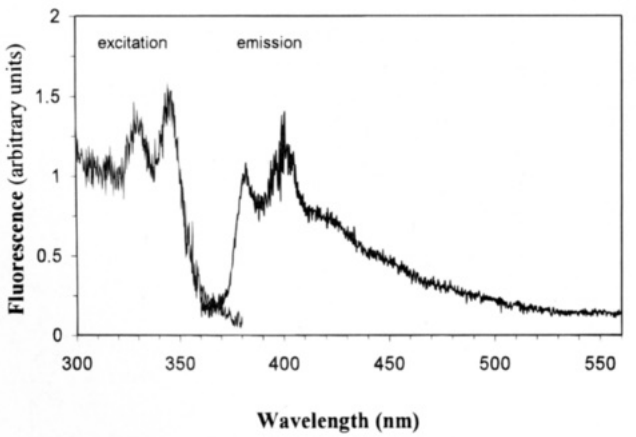

FIGURE 4: Fluorescence spectra of the (−)-*trans-anti*-BPDE−50-bp DNA construct. The excitation spectrum was recorded with emission at 400 nm, and the emission spectrum was recorded with excitation at 350 nm.

leads to dissociation of $UvrA_2$ from the $UvrA_2B$−DNA complex, resulting in formation of the UvrB−DNA complex. Nondamaged DNA did not support the formation of the UvrB−DNA complex. In addition, the appearance of the UvrB−DNA complex was only observed under conditions where ATP (1mM) and $MgCl_2$ (10 mM) were present in both the gel and the running buffer, suggesting their possible requirement for the stability of the complex (unpublished results). The composition of the proteins in these complexes were confirmed by Western analysis (data not shown) as previously described (Van Houten & Snowden, 1993).

DNase I Footprint of BPDE−DNA Complexes. DNase I footprinting experiments were performed to characterize the interactions of UvrA or UvrA/UvrB with BPDE−DNA lesions. Data displayed in Figure 6 indicate that DNase I digestion is sensitive to not only the protein−DNA complexes but also the stereochemistry of the BPDE-N^2 guanine adducts themselves.

Figure 6A shows the DNase I footprinting results for the 3′-end-labeled substrates in the absence of the repair proteins. Several interesting stereospecific patterns can be observed. In comparison to nondamaged DNA (lanes 2 and 3), (+)-*trans-anti*-BPDE−DNA surprisingly shows two hypersensitive sites flanking the modified residue in the footprint (lanes 5 and 6), but the (−)-*trans* isomer does not (Figure 6B, lane 4). Using the G and A + G Maxam−Gilbert sequencing products as a guide, the two sites have been found to be corresponding to phosphate cleavages between nucleotides $G_{25}G_{26}$ and $G_{26}G_{27}$ just next to the modified site G_{26} (summarized in Figure 7A). It should be noted that the

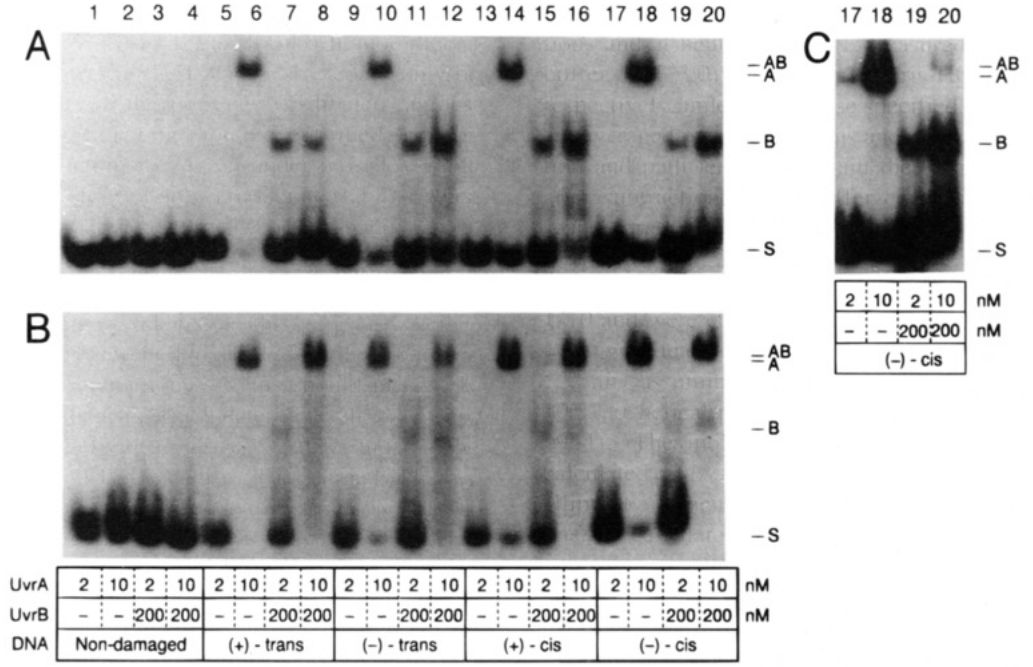

FIGURE 5: Binding of UvrA or UvrA/UvrB to the BPDE−DNA substrates. UvrA or UvrA/UvrB with the concentration as specified was incubated at 37 °C for 15 min with 1 nM BPDE−DNA substrates with the modified strand 5′-end-labeled and electrophoresed on both a 6% polyacrylamide (panels A and C) and 4% polyacrylamide (panel B) native gel in the presence of 1 mM ATP and 10 mM $MgCl_2$. Labels AB, A, and B represent the formation complexes of $UvrA_2B$, $UvrA_2$, and UvrB with the substrate, respectively. The S denotes the substrate free of proteins. Panel C is an overexposed autoradiograph of lanes 17−20 of panel A.

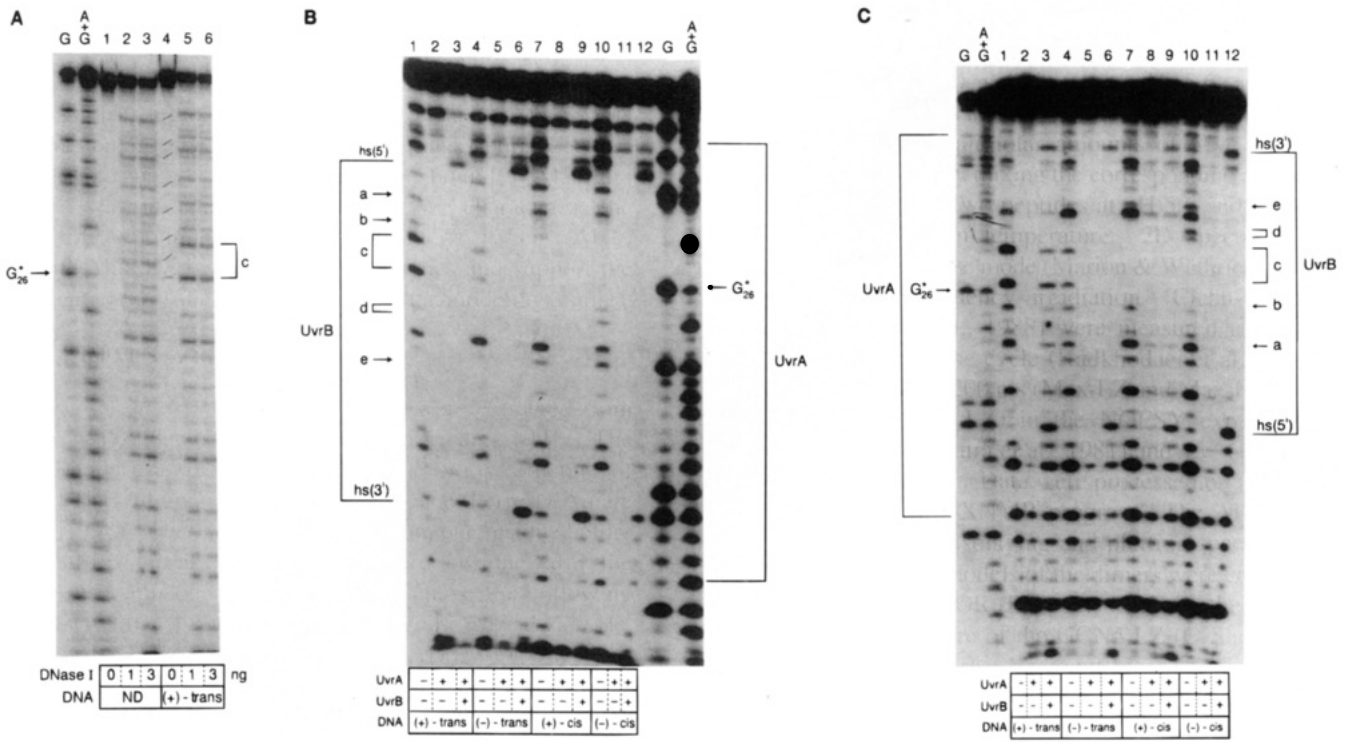

FIGURE 6: DNase I footprinting of BPDE−DNA and Uvr proteins−BPDE−DNA. The 5′- or 3′-terminally-labeled 50-bp DNA (2 nM) was incubated with UvrA (50 nM) or UvrA/UvrB (10 and 200 nM, respectively) at 37 °C for 15 min and then subjected to the digestion of DNase I (1 ng) in the presence of 0.1 M $CaCl_2$ at room temperature for 1 min. Panel A: DNase I footprint of nondamaged and (+)-*trans* BPDE adduct (3′-end-labeled). The lines (drawn in lane 4) between bands of nondamaged and damaged substrates indicate the digested DNA fragments with the same length and sequence. The migration difference is the result of retardation by pyrenyl moiety. Panel B: footprints of 3′-end-labeled BPDE−DNA and Uvr proteins interacting with these adducts. Panel C: the 5′-terminally-labeled substrates experimented as the same as in panel B. In all panels, lanes G and A+G represent Maxam−Gilbert sequencing products which were obtained with the (+)-*cis* BPDE substrate. Label G^*_{26} indicates the BPDE-modified guanine in the sequence. Brackets UvrA and UvrB show the footprints of UvrA and UvrB proteins interacting with the adducts, respectively. The hs(3′) and hs(5′) indicate the 3′-side and 5′-side DNase I hypersensitive sites, respectively. Bracket c indicates the lesion-induced DNase I hypersensitive sites and the shifted distance of the retardation by the BPDE group.

Maxam−Gilbert sequencing products were prepared with a BPDE modified substrate, and the band identifying a specific base in the sequence is actually a 3′-terminally-labeled fragment in which the specified nucleotide has been destroyed, leaving the 3′ phosphate. Comparison among the four stereoisomers indicates that the *trans*-BPDE adducts

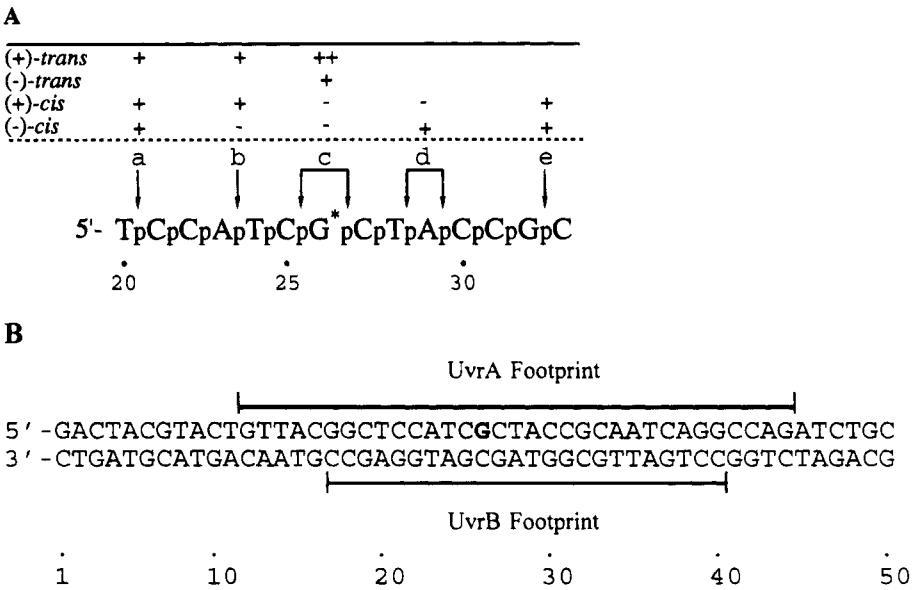

FIGURE 7: Schematic demonstration of DNase I footprint of BPDE adducts and UvrA and UvrB subunits. Panel A: alternation in DNase I cleavage patterns due to [BPDE]−DNA adducts. G*, the modified base. Labels +, ++, and − refer to DNase I sensitive, hypersensitive, and fully inhibited sites, respectively. Labels a−e are defined as in Figure 6. Panel B: DNase I footprinting sequences of UvrA and UvrB. The bold G refers to the modified base.

result in little or no inhibition of DNase I activity at or near the modified site (Figure 6B,C, lanes 1, 4, 7, and 10, summarized in Figure 7A), but the *cis*-BPDE adducts lead to clear DNase I footprints and complete inhibition to the enzyme activity at the lesion site. Other features which are stereospecific are indicated by arrows a through d (Figure 6B,C) and are summarized in Figure 7A.

The DNase I footprints produced by the interaction of UvrA or $UvrA_2UvrB$ with the 3′- and 5′-terminally-labeled (top strand) BPDE-damaged DNA are shown in Figure 6B,C, respectively. The G_{26}* indicates the modified nucleotide in the sequence, and c indicates the lesion-effecting region on DNase I digestion. As a control no footprints were observed when an identical nondamaged 50-bp DNA duplex was mixed with the Uvr proteins under the same conditions (data not shown). $UvrA_2$ when bound to either of the four substrates generates the same size footprint which covers a region of 33 bp from nucleotide G_{12} to C_{44} (top strand) (Figure 6B, lanes 2, 5, 8, and 11; Figure 6C). The same results have been obtained with 5′- or 3′-end-labeled substrates. Gel mobility shift studies indicated that the formation of UvrB−DNA intermediate strongly depends on the relative concentrations of UvrA with UvrB (see Figure 5). UvrA, at fixed concentrations (1 nM), when titrated with increasing UvrB (5−1000 nM), results in a continued increase of UvrB−DNA complex and a decrease of $UvrA_2B$−DNA (data not shown). In addition, the formation of the UvrB−DNA intermediate can be reversed by sufficiently high UvrA concentrations (when the UvrB:UvrA ratio becomes less than 10−15). With this understanding, appropriate concentrations of UvrA and UvrB have been used for the DNase I footprinting studies to reduce the formation of $UvrA_2B$−DNA so that the UvrB−DNA complex could be identified. As shown in Figure 6B,C, interaction of UvrA (10 nM) and UvrB (200 nM) with the damaged DNA (1 nM) generates a footprint for UvrB−DNA characterized by an area of 24-bp nucleotides encompassed by 5′- and 3′-hypersensitive sites, designated by hs(5′) and hs(3′), respectively (lanes 3, 6, 9, and 12). These results are summarized in Figure 7B.

UvrABC Incision of BPDE−DNA Adducts. Figures 8 and 9 show UvrABC incision of (+)-*trans*-, (−)-*trans*-, (+)-*cis*-, and (−)-*cis*-*anti*-BPDE-damaged 50-bp duplexes which were 5′- and 3′-terminally- labeled, respectively. The assay was performed with 1 nM DNA substrate, 10 nM UvrA, 100 nM UvrB, and 5 nM UvrC in UvrABC buffer (see Materials and Methods) incubated at 37 °C for 0−20 min. Since UvrA can dissociate from DNA after UvrB has come in contact with the damaged base and since the stability of UvrB−DNA preincision complex depends on the UvrA concentration, UvrA concentration was chosen to produce the maximum rate and extent of incision as determined in a UvrA titration experiment (data not shown).

Figure 8A,B demonstrates the UvrABC nuclease incision of the four BPDE-damaged 5′-terminally-labeled DNA substrates as a linear function of incubation time. The UvrABC nuclease incised all of the BPDE-adducted duplexes at the same position, the eighth phosphate 5′ to the modified guanine (Figure 8A). However, the rate and extent of incision vary with each stereoisomer. It is important to note that DNA fragments resulting from the endonuclease action contain a 3′ OH and migrate approximately one nucleotide more slowly than fragments of identical length with a 3′ phosphate generated by Maxam−Gilbert chemistry (Van Houten *et al.*, 1987). In addition, observation of the unmodified 50mer (Figure 8A, lanes 1, 6, and 11) migrating more rapidly than those modified is expected because the uncharged BPDE adduct (~300 Da) retards the migration to some extent. Figure 8B shows the results of four independent experiments in which the rate of substrate incision (m = fmol/min) has been determined by linear least-squares fitting. Of the four BPDE−DNA adducts surveyed, under the present experimental conditions, it is interesting to note that the (+)-*cis*-BPDE−DNA results in the highest incision rate, followed by (+)-*trans*-, (−)-*cis*-, and (−)-*trans*. A 4- or 5-fold difference is observed between the (+)-*cis* and (−)-*trans* stereoisomers, and the latter shows a surprisingly low incision efficiency. As a control the UvrABC nuclease did not incise the nondamaged duplex (Figure 8A, lanes 1, 6, and 11).

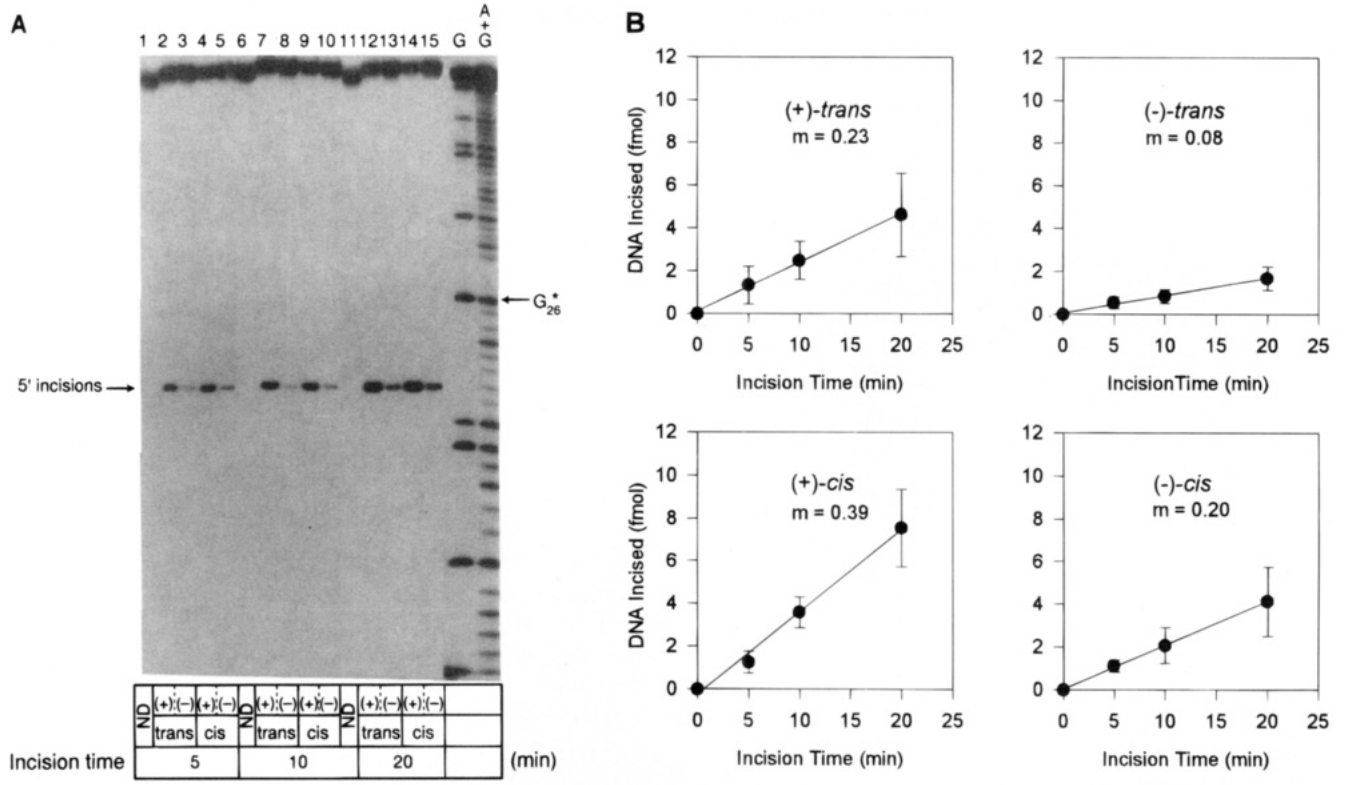

FIGURE 8: Incision of 5′-end-labeled BPDE-damaged 50-bp duplexes by UvrABC nuclease. [BPDE]−DNA (1 nM) was incubated with UvrA (10 nM), UvrB (100 nM), and UvrC (5 nM) in the UvrABC buffer at 37 °C for the indicated period. The incised products were then identified on a 12% polyacrylamide sequencing gel. Panel A: sequencing gel of incision products of substrates. Lanes 1, 6, and 11: nondamaged DNA assayed under the same conditions as others. Lanes 2, 7, and 12: (+)-*trans*-DNA incised for 5, 10, and 20 min, respectively. Lanes 3, 8, and 13: (−)-*trans* incised for 5, 10, and 20 min, respectively. Lanes 4, 9, and 14: (+)-*cis* incised for 5, 10, and 20 min, respectively. Lanes 5, 10, and 15: (−)-*cis* incised for 5, 10, and 20 min, respectively. G and A+G: Maxam−Gilbert sequencing products. G^*_{26} indicates the modified residue. Panel B: incision kinetics of BPDE−DNA substrates. Data are the mean ±sd of four independent experiments. The incision rate (referred to as *m*) is the slope of the line obtained from unweighted linear regression.

In comparison to the 5′-side incision, the 3′-side incision of BPDE−DNA adducts by UvrABC nuclease shows different patterns (Figure 9A). The most striking feature observed for the 3′-side incision is probably that each of the BPDE−DNA adducts offers a different spectrum of incision sites (Figure 9B). Instead of cleaving at only one site as on the 5′-side, the nuclease incises the substrates at three sites on the 3′-side of the modified guanine, five, six, and seven phosphates 3′ toward the modified site. Quantitation of the 3′ incisions by summing the amounts of cleavage from all the 3′-sites (P5, P6, and P7) shows results consistent with the 5′-side incisions of all four BPDE−DNA enantiomers; the incision efficiency is conserved with (+)-*cis*- > (+)-*trans*- ≥ (−)-*cis*- ≫ (−)-*trans*-. As shown in Figure 9A,B, UvrABC nuclease incises (+)-*trans*-*anti*-BPDE−DNA predominantly at phosphate 5 (P5) with minor incisions at two other sites. Interestingly, for the (−)-*trans*-BPDE-N^2-guanine adduct, cleavage at P5 is significantly reduced and that at P6 is slightly elevated as compared to the (+)-*trans* isomer. The incision a with one-nucleotide shift to the 3′-end seems to be consistent with the fact that the pyrene ring of the (−)-*trans* lesion is oriented toward the 3′-end of the modified DNA strand. The (+)-*cis* is cleaved predominately at phosphate five with almost no digestion at phosphate seven. For (−)-*cis*-BPDE−DNA, an incision is observed at phosphate seven, besides a major digestion product at phosphate five.

DISCUSSION

It is generally believed that the UvrABC nuclease system recognizes conformational changes in the DNA and not the modified base *per se*, but this hypothesis has never been tested directly. Data presented in this paper unambiguously show that the UvrABC nuclease system does in fact respond differently to four stereospecific adducts of BPDE which differ from one another in their stereochemical and conformational characteristics. These functional differences are discussed with respect to the known differences in the orientation and conformation of the four stereoisomers of *anti*-BPDE-N^2-guanine adducts.

Interaction of the UvrA and UvrB Proteins with BPDE−DNA Adducts. The gel mobility shift experiments demonstrate the formation of three protein−DNA complexes between BPDE-damaged DNA and the DNA repair proteins and are consistent with (1) the $UvrA_2$−DNA complex that forms predominately on damaged DNA, (2) the $UvrA_2B$−DNA complex that also forms predominately on damaged DNA, and (3) the UvrA-dependent UvrB−DNA complex that is only formed on damage-containing DNA. The exclusive formation of UvrB−DNA complex on lesions implies a direct role of UvrB−DNA in the efficient recognition of DNA damage. While our gel mobility shift assays were generally successful, it should be noted that the efficiency of formation of $UvrA_2B$ and UvrB−DNA complexes in the gels is markedly affected by the polyacrylamide concentration: for example, $UvrA_2B$ complex formation is favored in 4% polyacrylamide gels (Figure 5).

Footprints of UvrA and UvrB have been previously reported for many different types of lesions (Van Houten *et al.*, 1987; Visse *et al.*, 1992; Snowden & Van Houten, 1991; Bertrand-Burggraf *et al.*, 1991). Consistent with these earlier

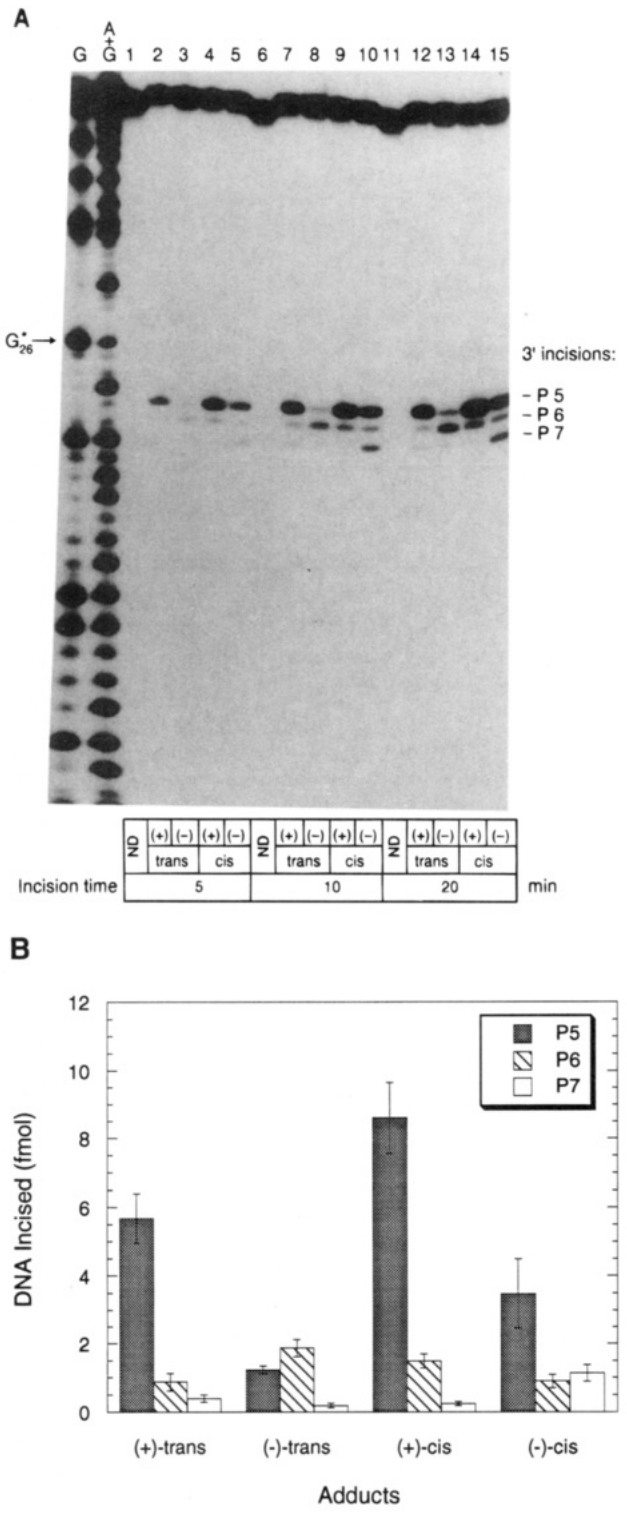

FIGURE 9: Incision of 3′-end-labeled BPDE-damaged 50-bp duplexes by UvrABC nuclease. [BPDE]−DNA (1 nM) was incubated with UvrA (10 nM), UvrB (100 nM), and UvrC (5 nM) in the UvrABC buffer at 37 °C for the indicated period. The incised products were then identified on a 12% polyacrylamide sequencing gel. Panel A: sequencing gel of incision products of substrates. G^*_{26} indicates the modified residue. P5, P6, and P7 indicate the fifth, sixth, and seventh backbone phosphates 3′ toward the modified guanine. G and A+G: Maxam−Gilbert sequencing products. Lanes 1, 6, and 11: nondamaged DNA tested under the same conditions as others. Lanes 2, 7, and 12: (+)-*trans*-DNA incised for 5, 10, and 20 min, respectively. Lanes 3, 8, and 13: (−)-*trans* incised for 5, 10, 20 min, respectively. Lanes 4, 9, and 14: (+)-*cis* incised for 5, 10, and 20 min, respectively. Lanes 5, 10, and 15: (−)-*cis* incised for 5, 10, and 20 min, respectively. Panel B: graphic plot of the incision. Data were plotted as the mean of three independent experiments. Error bars show the standard deviation.

studies, UvrA, presumably as a dimer, interacts with the BPDE-adducted 50-bp duplexes protecting a region of 28−33 bp from DNase I digestion, and UvrB, when bound to DNA, protects a 24-bp region from DNase I digestion.

These qualitative studies did not reveal any differences in the binding of $UvrA_2$ or $UvrA_2B$ to the four stereoisometric lesions of BPDE. It will be interesting to determine whether specific binding of either protein may correlate to rates of incision, as has been suggested previously (Visse *et al.*, 1992), and whether UvrC may play an important role in damage recognition.

Effect of BPDE Conformation on Incision Sites. Tang *et al.* (1992), using DNA fragments randomly damaged with a racemic mixture of (±)-*anti*-BPDE, have previously shown that the UvrABC nuclease incises the eighth phosphate 5′ and primarily the fifth and sometimes the sixth phosphate 3′ to BPDE-modified guanines. The results obtained here with site-specific and stereochemically defined adducts derived from the covalent binding of the (+)- and (−)-*anti*-BPDE enantiomers to DNA generally confirm this pattern; however, both qualitative and quantitative differences in the incision patterns and efficiencies of the UvrABC nuclease activities are observed. It is believed that the dual incisions are performed by the action of UvrB on the 3′-side followed by UvrC-mediated cleavage on the 5′-side of the damaged nucleotide (Linn & Sancar, 1992). Results presented here in which cleavage occurs primarily at the fifth and also at the sixth and seventh phosphates 3′ to the BPDE-N^2-guanine adducts suggest that UvrB is a flexible protein which adapts its conformation to the feature of lesions. In contrast, the UvrC protein appears to lack this type of conformational flexibility as the 5′ incision site occurred at the eighth phosphate 5′ in all four cases. It is interesting to note that the DNase I footprints and hypersensitive sites for the UvrB−DNA complex are essentially identical for the (+)-*trans*- and (−)-*trans*-BPDE-N^2-guanine adducts (Figures 6 and 7), even though the presumed UvrB-mediated 3′ incision is shifted one nucleotide 3′ for the (−)-*trans*-BPDE-N^2-guanine adduct, such that cleavage occurs predominately at the sixth phosphate. To accommodate the new incision site it might be expected that the hypersensitive sites would be shifted one nucleotide 3′; however, this appears not to be the case. Two important questions arise from the experiments described in this work: (1) why does UvrABC incise (+)-isomers better than the corresponding (−)-isomers, and (2) why does UvrABC incise (+)-*cis* stereoisomeric adduct better than the other three. The results presented here, together with the known conformational (Cosman *et al.*, 1992, 1993; de los Santos *et al.*, 1992) and other physical characteristics (Ya *et al.*, 1994; Xu and Geacintov, unpublished results), provide a basis for addressing these questions.

BPDE−DNA Adduct Recognition and Repair: Structure−Function Relationships. The structures of three of the four stereoisomer BPDE−DNA adducts used in this study have been determined by 2D-NMR techniques in conjunction with distance-constrained energy minimization (Figure 10). In the (+)-*trans* and (−)-*trans* adducts the bulky pyrenyl residue fits neatly into the minor groove, with little perturbation of the B-DNA double helix, and points in opposite directions relative to the modified guanine residues (Cosman *et al.*, 1992). In contrast, the intercalative binding mode of the (+)-*cis* (Cosman *et al.*, 1993) and (−)-*cis* isomers (M. Cosman *et al.*, to be published) leads to rupture of the modified guanine and cytidine base pair, such that in the case of the

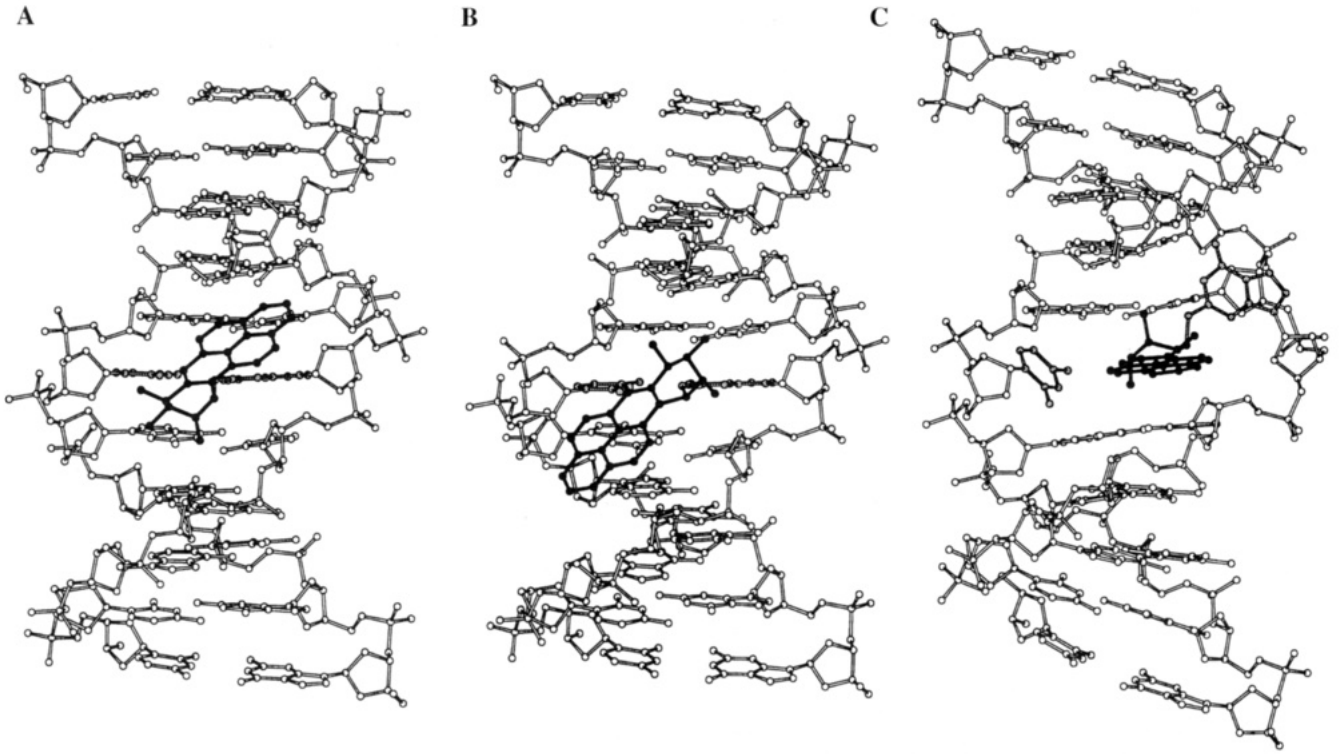

FIGURE 10: Molecular models of the (+)-*trans*-, (−)-*trans*-, and (+)-*cis*-*anti*-BPDE−DNA substrates (A−C, respectively) based on energy minimization calculations using 2D-NMR NOE-derived distance constraints from Cosman *et al.* (1992, 1993) and de los Santos *et al.* (1992). The view is looking into the minor groove. The pyrenyl moiety is black, and the modified G and corresponding C are gray.

(+)-*cis* isomer the guanine and cytidine rings are swung out into the minor and major grooves, respectively. Analysis of the BPDE-modified DNA duplexes using DNase I footprinting suggests that this enzyme is an excellent probe for assessing the conformational and structural alterations induced by the different stereoisomeric BPDE−DNA adducts (Figures 6A−C and 7A). For example, the (+)-*cis*-BPDE-N^2-guanine adduct leads to a large footprint (Figure 6B, lane 7), whereas the (−)-*trans*-BPDE-N^2-guanine adduct generates little, if any, footprint (Figure 6B, lane 4). These DNase I footprinting results are consistent with the UvrABC nuclease system incision efficiency for these two BPDE−DNA adducts.

It has been suggested that the UvrABC nuclease complex generally recognizes a localized DNA helix alteration including bending, kinking, and unwinding rather than a specific modified nucleotide [Van Houten *et al.*, 1986; Walter *et al.*, 1988; and reviewed in Van Houten (1990)]. The BPDE−DNA adducts have different effects on the thermostability of 11mer duplexes such that the T_m of the unmodified 11mer is 50.5 °C, whereas the T_m's for the (+)- and (−)-*trans* isomers are 40 and 43.2 °C, respectively (Ya *et al.*, 1994). The two *cis* isomers have slightly higher T_m's (46 °C); thus, the loss of hydrogen bonding between the BPDE-modified guanine and its partner cytidine residue is partially offset by pyrenyl residue base-stacking interactions (Cosman *et al.*, 1993). Since the UvrABC system incises the *cis* isomers more efficiently than the corresponding *trans* isomers, it appears that the enzyme complexes recognize the distorted base-displaced intercalative *cis*-adduct structures more readily than the minor groove *trans*-adduct conformations which are minimally distorted. The differences in the thermal stabilities, which are measures of the deviations of the thermodynamic characteristics of the modified duplexes from those of the normal duplexes, appear to be less important for recognition.

Features of DNA Damage That are Important for Efficient Recognition and Repair. The results presented here when combined with the previous database of DNA adducts recognized by the UvrABC nuclease system (Lloyd & Van Houten, 1995) lead to some general considerations of damage recognition. UvrABC-mediated damage recognition is a dynamic three-step cascade in which UvrA provides approximately 3 orders of specificity for damaged versus nondamaged DNA. This level of discrimination is imprecise as abasic sites which are poorly incised by the UvrABC nuclease are bound efficiently by the UvrA protein (Snowden & Van Houten, 1991). UvrA-mediated discrimination is probably different than UvrB, which provides increased specificity and stability. We have postulated that UvrB, in a second level of discrimination, uses hydrophobic stacking interactions between the aromatic amino acid side chains and the bases to promote this specificity (Van Houten & Snowden, 1993). Thus we propose that intercalation-type lesions such as the (+)-*cis*-BPDE-N^2-guanine might stabilize the formation of the preincision UvrB−DNA complex and promote efficient incision, whereas minor groove conformers, such as the (−)-*trans*-BPDE-N^2-guanine adduct, are not recognized as efficiently. In support of the hypothesis that UvrB is involved in damage recognition by making intimate contacts with the damaged base, we have shown that UvrB can be directly cross-linked to bis(platinum)−DNA adducts (Van Houten *et al.*, 1993). This hypothesis is also supported by recent studies emerging from the Sancar laboratory (Hsu *et al.*, 1995) which show that UvrB in the absence of UvrA can interact directly with damaged nucleotides in single-stranded DNA. These studies strongly suggest that UvrB is an active player in damage recognition and is not merely loaded by UvrA (Sancar & Hearst, 1992). UvrA together with UvrB work through a limited helicase activity to examine the DNA helix from the inside−out by probing base-stacking interactions. UvrB binding appears to promote

DNA bending, and, since DNA unwinding and bending are energetically linked (Ramstein & Lavery, 1988), any DNA adduct that bends and unwinds the helix should promote the formation of the UvrB−DNA preincision complex. This nicely explains why the (+)-*trans*-BPDE-N^2-guanine isomer which causes a dynamic bend is incised more efficiently than the (−)-*trans*-isomer (Xu and Geacintov, unpublished observation). A final level of discrimination occurs when UvrC binds to the UvrB−DNA preincision complex. This binding induces an allosteric change in the UvrB, activating a nuclease, which is believed to incise the DNA 3′ to the damaged base. Thus adducts such as the (−)-*trans*-BPDE-N^2-guanine which lie in the minor groove in the 3′ direction can inhibit the incision reaction.

Potential Biological Implications of Slow Repair of (−)-trans-BPDE Adducts. Studies on translesional synthesis *in vitro* with DNA templates containing stereospecific BPDE adducts and PolI Klenow fragment indicated that (−)-*anti*-BPDE−DNA has much higher miscoding potential dominated by G → T transversions or deletions than the (+)-*anti*-BPDE isomers (Shibutani *et al.*, 1993). It is clear that failure to repair such DNA damage could result in mutagenicity, and, ultimately, a series of appropriate mutations could result in tumorigenicity (or cancer). In fact, BPDE-induced G → T transversions are dominant in the mutation spectra of several types of mammalian cells (Yang *et al.*, 1987; Mazur & Glickman, 1988; Carothers & Grunberger, 1990; Chen *et al.*, 1990, 1991; Keohavong & Thilly, 1992) and in bacteria (Mizusawa *et al.*, 1981; Eisenstadt *et al.*, 1982; Bernelot-Moens *et al.*, 1990). Also, high-frequency base deletions induced by BPDE have also been observed (Mizusawa *et al.*, 1981; Chakrabarti *et al.*, 1984; Yang *et al.*, 1987; Roilides *et al.*, 1988; Bernelot-Moens *et al.*, 1990). The relatively low incision rate of (−)-*trans-anti*-BPDE−DNA by UvrABC nuclease under the conditions used in the present study could help explain the higher mutation frequency of this BPDE isomer in *Salmonella* (Wood *et al.*, 1977; Steven *et al.*, 1985).

CONCLUSIONS

Although BPDE-N^2-guanine stereoisomers have the same chemical formula and are distinct from each other only by their three-dimensional configurations, their biological consequences, including mutagenicity and carcinogenicity, are greatly different. It is widely accepted that DNA repair can be an important factor in mutagenesis since lesions that are rapidly repaired have a smaller probability of expressing their mutagenic potential as compared to those that are repaired more slowly. Since the structural differences of these lesions result from and only from differences in the stereochemical addition of the BPDE moiety to the N^2-position of guanine, the characterization of the UvrABC system with these lesions provides a better understanding of the damage recognition mechanism of UvrABC nuclease. This study gave direct evidence that the *cis*-BPDE intercalative base displacement adducts are recognized more efficiently than the *trans* minor groove binding isomers.

Results presented here clearly show that the UvrABC nuclease system inspects the conformational parameters of the DNA helix rather than the modified bases per se.

Future studies will examine the steps leading up to incision, UvrA binding, and the formation of the UvrAB−DNA complex and its transition to UvrB−DNA.

ACKNOWLEDGMENT

We thank Dr. Shantu Amin (American Health Foundation, Valhalla, NY) for the synthesis of the optically pure BPDE isomers, Dr. Monique Cosman for the computer-generated models used in Figure 10, Dr. David A. Scicchitano (Department of Biology, NYU) for helpful assistance during the early phases of this project, Dr. Amal Kumar for helping us develop a new UvrA purification scheme, and Heather Bassett for purifying UvrA. We would also like to thank Dr. Randy Walker and Heather Bassett for critical reading of the manuscript.

REFERENCES

Bernelot-Moens, C., Glickman, B. W., & Gordon, A. J. (1990) *Carcinogenesis 11,* 781−785.
Bertrand-Burggraf, E., Selby, C. P., Hearst, J. E., & Sancar, A. (1991) *J. Mol. Biol. 219,* 27−36.
Buening, M. K., Wislocki, P. G., Levin, W., Yagi, H., Thakker, D. R., Akagi, H., Koreeda, M., Jerina, D. M., & Conney, A. H. (1978) *Proc. Natl. Acad. Sci. U.S.A. 75,* 5358−5361.
Burgess, J. A., Stevens, C. W., & Fahl, W. E. (1985) *Cancer Res. 45,* 4257−4262.
Carothers, A. M., & Grunberger, D. (1990) *Carcinogenesis,* 189−192.
Chakrabarti, S., Mizusawa, H., & Seidman, M. (1984) *Mutat. Res. 126,* 127−137.
Chen, R.-H., Maher, V. M., & McCormick, J. J. (1990) *Proc. Natl. Acad. Sci. U.S.A. 87,* 8680−8684.
Chen, R.-H., Maher, V. M., & McCormick, J. J. (1991) *Cancer Res. 51,* 2587−2592.
Choi, D. J., Marino-Alessandri D. J., Geacintov, N. E., & Scicchitano, D. A. (1994) *Biochemistry 33,* 780−787.
Cosman, M., Geacintov, N. E., & Amin, S. (1991) in *Proceedings of the 13th International Symposium on Polynuclear Aromatic Hydrocarbons,* Bordeaux, France, October 1−4, 1991 (Garrigues, P., & Lamotte, M., Eds.) pp 1151−1158, Gordon and Breach Science Publishers, New York.
Cosman, M., de los Santos, C., Fiala, R., Hingerty, B. E., Singh, S. B., Ibanez, V. Margulis, L. A., Live, D., Geacintov, N. E., Broyde, S., & Patel, D. J. (1992) *Proc. Natl. Acad. Sci. U.S.A. 89,* 1914−1918.
Cosman, M., de los Santos, C., Fiala, R., Hingerty, B. E., Ibanez, V., Luna, E., Harvey, R., Geacintov, N. E., Broyde, S., & Patel, D. J. (1993) *Biochemistry 32,* 4146−4155.
de los Santos, C., Cosman, M., Hingerty, B. E., Ibanez, V. Margulis, L. A., Geacintov, N. E., Broyde, S., & Patel, D. J. (1992) *Biochemistry 31,* 5245−5252.
Eisenstadt, E., Warren, J., Porter, J., Atkins, D., & Miller, J. (1982) *Proc. Natl. Acad. Sci. U.S.A. 79,* 1945−1949.
Geacintov, N. E., Gagliano, A. G. Ibanez, V., & Harvey, R. G. (1982) *Carcinogenesis 3,* 247−253.
Geacintov, N. E., Cosman, M., Ibanez, V., Birke, S. S., & Swenberg, C. E. (1990) in *Molecular Basis of Specificity in Nucleic Acid−Drug Interactions* (Pullman, B., & Jortner, J., Eds.) pp 443−450, Kluwer Academic Publishers, Dordrecht, The Netherlands.
Geacintov, N. E., Cosman, M., Mao, B., Alfano, A., Ibanez, V., & Harvey, R. G. (1991) *Carcinogenesis 12,* 2099−2108.
Grossman, L., & Thiagalingam, S. (1993) *J. Biol. Chem. 268,* 16871−16874.
Hruszkewycz, A. M., Canella, K. A., Peltonen, K., Kotrappa, L., & Dipple, A. (1992) *Carcinogenesis 13,* 2347−2352.
Hsu, D. S., Kim, S.-T., Qing, S., & Sancar, A. (1995) *J. Biol. Chem. 270,* 8319−8327.
Keohavong, P., & Thilly, W. G. (1992) *Proc. Natl. Acad. Sci. U.S.A. 89,* 4623−4627.
Koo, H.-S., Classen L., Grossman L., & Liu, L. F. (1991) *Proc. Natl. Acad. Sci. U.S.A. 88,* 1212−1216.
Lin, J.-J., & Sancar, A. (1992) *J. Biol. Chem. 267,* 17688−17692.
Lin, J.-J., Phillips, M., Hearst, J. E., & Sancar, A. (1992) *J. Biol. Chem. 267,* 17693−17700.
Lloyd, R. S., & Van Houten, B. (1995) DNA Damage Recognition, in *DNA Repair Mechanisms: Impact on Human Diseases and*

Cancer (Vos, J.-M., Ed.) R. G. Landes Company Biomedical Publishers, Austin, TX (in press).
Maxam, A. M., & Gilbert, W. (1980) *Methods Enzymol. 65,* 499–560.
Mazur, M., & Glickman, B. W. (1988) *Somatic Cell Mol. Genet. 14,* 393–400.
Mazur, S. J., & Grossman, L. (1991) *Biochemistry 30,* 4432–4443.
Mizusawa, H., Lee, C.-H., Kakefuda, T., Mckenney, K., Shimatake, H., & Rosenberg, M. (1981) *Proc. Natl. Acad. Sci. U.S.A. 78,* 6817–6820.
Moolenaar, G. F., Visse, R., Ortiz-Buysse, M., Goosen, N., & van de Putte, P. (1994) *J. Mol. Biol. 240,* 294–307.
Myles, G. M., & Sancar, A. (1991) *Biochemistry 30,* 3834–3840.
Oh, E. Y., & Grossman, L. (1986) *Nucleic Acids Res. 14,* 8557–8571.
Oh, E. Y., & Grossman, L. (1989) *J. Biol. Chem. 264,* 1336–1343.
Orren, D. K., & Sancar, A. (1989a) *Proc. Natl. Acad. Sci. U.S.A. 86,* 5237–5241.
Orren, D. K., & Sancar, A. (1989b) in *Mechanisms and Consequences of DNA Damage Processing, UCLA Symposia on Molecular and Cellular Biology, New Series* (Friedberg, E., & Hanawalt, P., Eds.) Vol. 83, pp 87–94, Alan R. Liss, Inc., New York.
Orren, D. K., & Sancar, A. (1990) *J. Biol. Chem. 265,* 15796–15803.
Ramstein, J., & Lavery, R. (1988) *Proc. Natl. Acad. Sci. U.S.A. 85,* 7231–7235.
Rodriguez, H., & Loechler, E. L. (1993) *Biochemistry 32,* 1759–1769.
Roilides, E., Gielen, J. E., Tuteja, N., Levine, A. S., & Dixon, K. (1988) *Mutat. Res. 198,* 199–206.
Sancar, A., & Rupp, W. D. (1983) *Cell 33,* 249–260.
Sancar A., & Hearst, J. E. (1993) *Science 259,* 1415–1420.
Sancar, A., Thomas, D. C., Van Houten, B., Husain, I., & Levy, M. (1987) in *DNA Repair, A Laboratory Manual of Research Procedures* (Friedberg, E. C., & Hanawalt, P. C., Eds.) Vol. 3, Chapter 24, pp 479–508, Marcel Deckker, New York.
Shibutani, S., Margulis, L. A., Geacintov, N. E., & Grollman, A. P. (1993) *Biochemistry 32,* 7531–7541.
Slaga, T. J., Bracken, W. J., Gleason, G., Levin, W., Yagi, H., Jerina, D. M., & Conney, A. H. (1979) *Cancer Res. 394,* 67–71.
Snowden, A., & Van Houten, B. (1991) *J. Mol. Biol. 220,* 19–33.
Stevens, C. W., Bouck, N., Burgess, J. A., & Fahl, W. F. (1985) *Mutat. Res. 152, 5–14.*
Tang, M., Pierce, J. R., Doisy, R. P., Nazimiec, M. E., & MacLeod, M. C. (1992) *Biochemistry 31,* 8429–8436.
Van Houten, B. (1990) *Microbiol. Rev. 54,* 18–51.
Van Houten, B., & Snowden, A. (1993) *BioEssays 15,* 51–59.
Van Houten, B., & McCullough, A. (1994) in *DNA Damage Effects on DNA Structure and Protein Recognition* (Wallace, S. S., Van Houten, B., & Kow, Y. W., Eds.) pp 236–251, The New York Academy of Sciences, New York.
Van Houten, B., Gamper, H., Sancar, A., & Hearst, J. E. (1987) *J. Biol. Chem. 262,* 13180–13187.
Van Houten, B., Illenye, S. Yen, Q., & Farrel, N. (1993) *Biochemistry 32,* 11794–11801.
Visse, B., de Ruijter, M., Moolenaar, G. F., & van de Putte, P. (1992) *J. Biol. Chem. 267,* 6736–6742.
Walter, R. B., Rierce, J., Case, R., & Tang, M.-S. (1988) *J. Mol. Biol. 203,* 939–947.
Wei, S.-J. C., Chang, R. L., Hennig, E., Cui, X. X., Merkler, K. A., Wong, C.-Q., Yagi, H., & Conney, A. H. (1994) *Carcinogenesis 15,* 1729–1735.
Wood, A. W., Chang, R. L., Levin, W., Yagi, H., Thakker, D. R., Jerina, D. M., & Conney, A. H. (1977) *Biochem. Biophys. Res. Commun. 77,* 1389–1396.
Xu, R., Birke, S., Carberry, S. E., Geacintov, N. E., Swenberg, C. E., & Harvey, R. G. (1992) *Nucleic Acids Res. 20,* 6167–6176.
Ya, N. Q., Smirnov, S., Cosman, M., Bhanot, S., Ibanez, V., & Geacintov, N. E. (1994) in *Structural Biology: The State of the Art* (Sarma, R. H., & Sarma, M. H., Eds.) pp 349–366, Adenine Press, Guilderland, NY.
Yang, J.-L., Maher, V. M., & McCormick, J. J. (1987) *Proc. Natl. Acad. Sci. U.S.A. 84,* 3787–3791.

BI951244C